

## Tuning and probing interfacial bonding channels for a functionalized organic molecule by surface modification

G. Mercurio,<sup>1,2,\*</sup> O. Bauer,<sup>3</sup> M. Willenbockel,<sup>1,2</sup> B. Fiedler,<sup>3</sup> T. Sueyoshi,<sup>1,2</sup> C. Weiss,<sup>1,2</sup> R. Temirov,<sup>1,2</sup> S. Soubatch,<sup>1,2</sup> M. Sokolowski,<sup>3</sup> and F. S. Tautz<sup>1,2</sup>

<sup>1</sup>*Peter Grünberg Institut (PGI-3), Forschungszentrum Jülich, 52425 Jülich, Germany*

<sup>2</sup>*Jülich Aachen Research Alliance (JARA), Fundamentals of Future Information Technology, 52425 Jülich, Germany*

<sup>3</sup>*Institut für Physikalische und Theoretische Chemie, Universität Bonn, 53115 Bonn, Germany*

(Received 31 October 2012; published 28 March 2013)

The potassium-induced missing row reconstruction of Ag(110) is used to selectively modify the local chemical interaction between the functional anhydride groups of 3,4,9,10-perylene-tetracarboxylic-dianhydride (PTCDA) and Ag(110). We find a significant upward shift of the anhydride groups, while the adsorption height of the perylene core is essentially preserved. This demonstrates an attractive perylene/substrate interaction for PTCDA/K:Ag(110), elucidating also the bonding situation for the potassium-free system.

DOI: [10.1103/PhysRevB.87.121409](https://doi.org/10.1103/PhysRevB.87.121409)

PACS number(s): 68.43.Fg, 61.05.jh, 68.37.Ef, 68.49.Uv

Organic/metal interfaces with tailor-made structural and electronic properties are currently the subject of an intense research effort.<sup>1–4</sup> Organic molecules with functional groups support multiple interactions, often referred to as different *bonding channels*, with a metal surface. While the individual bonding channels depend on the (chemical) affinity of the respective part of the molecule toward the substrate, the final geometric and electronic structure of the interface is determined by the interplay between the different bonding channels. To tailor interface properties it is therefore important not only to understand and control the individual channels, but also to take into account their subtle interdependence.

An example is provided by 3,4,9,10-perylene-tetracarboxylic-dianhydride (PTCDA) [Fig. 1(a)].<sup>5–11</sup> It interacts with Ag surfaces via two coupled bonding channels.<sup>12</sup> First, the oxygen atoms (primarily the carboxylic oxygens  $O_{\text{carb}}$ , and to a lesser extent the anhydride oxygens  $O_{\text{anhyd}}$ ) bond covalently to the Ag surface atoms underneath. Second, there is metal-to-molecule charge transfer involving the entire molecule,<sup>7,13,14</sup> which also leads to a partial rehybridization of the former lowest unoccupied molecular orbital (F-LUMO).<sup>15,16</sup> This results in a covalent bonding of the perylene core ( $C_{\text{peryl}}$ ) to the Ag substrate, which together with the van der Waals interaction forms the second bonding channel.<sup>17</sup> The charge transfer into the F-LUMO changes the molecule internally towards a quinodal structure,<sup>18</sup> hence increasing its structural flexibility and consequently reinforcing the local O-Ag interaction, with the result that the perylene core of the molecule is pulled even further towards the surface. The bonding of PTCDA to low index silver surfaces Ag(111),<sup>19–21</sup> Ag(100),<sup>12</sup> and Ag(110)<sup>22</sup> therefore involves a synergism of the two bonding channels mentioned above.<sup>12</sup> In fact, it has been suggested that the perylene core of PTCDA is pulled into the repulsive regime by the local O-Ag interaction, thus leading to the characteristic bending of the molecule<sup>12,22</sup> [Fig. 1(b)].

The above model has been derived on the basis of a systematic study of PTCDA bonding to the three canonical low index silver surfaces and explains the geometries and the electronic structure of the interfaces (including the silver atoms) qualitatively correctly. However, while the existence

of the O-Ag bonding channel is evident from the molecular distortion, the attractiveness of the  $C_{\text{peryl}}$ -Ag interaction<sup>13</sup> has not yet been proven directly by structural means. In the work reported here we provide this proof by selectively altering the O-Ag interaction and measuring whether and how the perylene core responds, in terms of its adsorption height. This also allows conclusions regarding the coupling of the two channels. We achieve this by selectively replacing in the Ag(110) surface the Ag atoms below the oxygens with another metal (potassium). By substituting metal atoms *locally only*, we keep the structure of the surface below the perylene core essentially unchanged, such that the results of our experiment also lead to a deeper understanding of the PTCDA bonding to the pure Ag(110) surface.

PTCDA molecules are evaporated from a Knudsen cell onto the Ag(110) substrate kept at room temperature, and subsequently annealed. Potassium is then deposited from a commercial SAES getter source and the sample is annealed again. Annealing temperatures and times, which depend on the sample holder geometry, are given in the Supplemental Material.<sup>23</sup> The K/PTCDA/Ag(110) interface is studied by a combination of high-resolution electron diffraction (SPA-LEED) and low-temperature ( $\approx 5$  K) scanning tunneling microscopy (STM) for lateral structure determination, normal-incidence x-ray standing waves (NIXSW) for vertical structures, x-ray photoelectron spectroscopy (XPS) for chemical analysis, and ultraviolet photoelectron spectroscopy (UPS) for work function and electronic structure measurements. NIXSW was carried out at beamline ID32 at the ESRF. UPS experiments were performed at the beamline U125/2-SGM at BESSY II and partly in the home lab. Note that the K/PTCDA/Ag(110) interfaces studied here are different from the multilayers reported in Refs. 24 and 25.

Alkali metals are known to induce a missing row reconstruction on fcc (110) metal surfaces; i.e., they substitute the substrate atomic rows.<sup>26,27</sup> In the case of K/Ag(110) it was observed that the surface reconstruction is a thermally activated process and that the period of the reconstructed surface depends on the amount of alkali metal deposited.<sup>28,29</sup> At the same time, potassium as electropositive atom interacts with the electronegative oxygen atoms of PTCDA molecules,

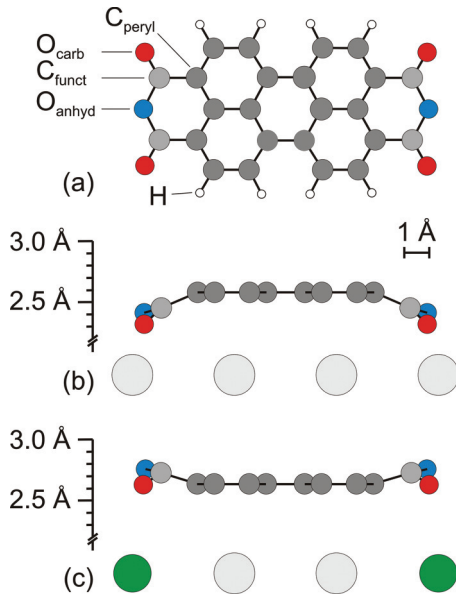


FIG. 1. (Color) (a) PTCDA molecule. (b), (c) Side view of one molecule and unrelaxed uppermost Ag layer of the PTCDA/Ag(110) brick-wall phase (Ref. 22) [panel (b)] and the PTCDA/K:Ag(110) stripe phase [panel (c)]. All vertical distances follow from NIXSW experiments (Ref. 23) (see Table I).

as confirmed by density functional theory calculations.<sup>31</sup> On the basis of these two facts, we expect it to be possible to substitute Ag atoms of Ag(110) below PTCDA oxygen atoms by potassium. This expectation is borne out by our results.

The thermodynamically stable phase of K/PTCDA/Ag(110) at the corresponding K coverage is the *stripe phase* [Fig. 2(a) left side, Figs. 2(d)–2(e)]. With a potassium coverage of 2–3 K atoms per PTCDA molecule, determined by XPS,<sup>23</sup> this phase can be prepared under LEED control as a homogeneous overlayer on the Ag(110) surface [Fig. 2(f)]. The stripe phase is a regular arrangement of bright and dark terraces, both covered by PTCDA molecules. A kinematic simulation<sup>23</sup> of the SPA-LEED data [Figs. 2(g) and 2(h)] indicates a unit cell with a length of 26 silver lattice constants in the [001] direction, consisting of a sequence of two PTCDA molecules on an up terrace (bright), two on a down terrace (dark), two on an up terrace, and one on a down terrace. Note that STM images, see, e.g., Fig. 2(a), reveal the presence of stacking faults which lead to local deviations from this sequence. The steps between the bright and dark terraces are monoatomic silver steps with the height of 1.44 Å.<sup>23</sup> The terraces are covered by PTCDA *monolayers*, as manipulation experiments in which molecules are removed from the terraces with the STM tip show.<sup>23</sup> Molecules order in a staggered arrangement perpendicular to the steps. The molecular layers exhibit the same order and internal contrast on the upper and lower terraces, revealing that the molecule-metal interface structure on both terraces is identical.

Although the appearance of the stripe phase is clearly correlated to the presence of potassium, the latter is not visible in STM images of the stripe phase. However, the visibility of individual K atoms in another phase, the *X phase*, where K atoms are imaged within the PTCDA layer [Fig. 2(c)], suggests that in the stripe phase K atoms are located in the

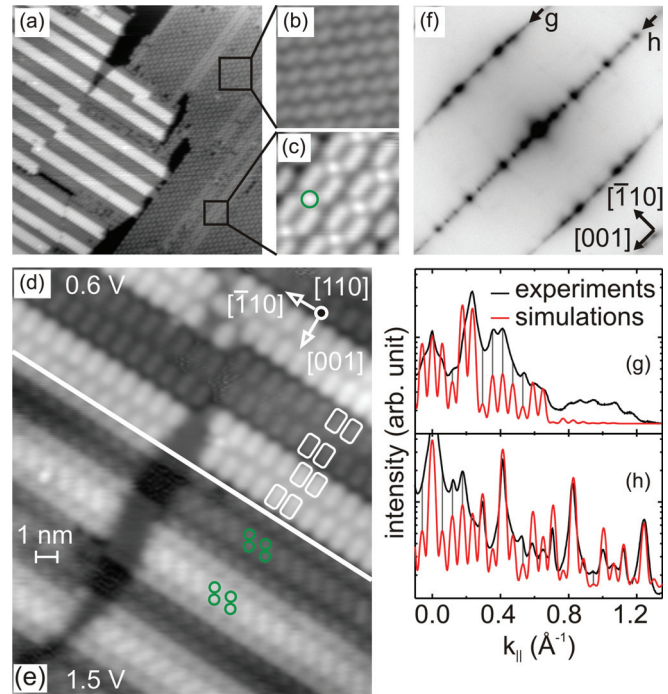


FIG. 2. (Color) (a) STM image of K/PTCDA/Ag(110) after annealing at 180 °C for 5 min. Image parameters:  $160 \times 160 \text{ nm}^2$ ,  $I = 55 \text{ pA}$ ,  $V = 0.6 \text{ V}$ . (b) PTCDA brick-wall phase. Image parameters:  $6.4 \times 6.4 \text{ nm}^2$ ,  $I = 0.4 \text{ nA}$ ,  $V = -0.3 \text{ V}$ . (c) K+PTCDA X phase. Green circle marks potassium. Image parameters:  $4.8 \times 4.8 \text{ nm}^2$ ,  $I = 1.1 \text{ nA}$ ,  $V = 0.6 \text{ V}$ . (d), (e) STM images of the stripe phase acquired with bias voltages  $V = 0.1 \text{ V}$ ,  $I = 1.0 \text{ nA}$  [panel (d)], and  $V = 1.5 \text{ V}$ ,  $I = 5.0 \text{ nA}$  [panel (e)]. Green circles in panel (e) mark K-induced features, white rectangles in panel (d) mark PTCDA molecules. (f) SPA-LEED image of a surface with a homogeneous stripe phase, measured with 24.5 eV electrons at 180 K. (g), (h) SPA-LEED line profiles (black) marked by the arrows in panel (f), and corresponding kinematic simulations (red) of the 2 up, 2 down, 2 up, 1 down pattern [superstructure matrix  $\begin{pmatrix} 3 & 0 \\ 0 & 26 \end{pmatrix}$ ] shown in Fig. 3.

surface, i.e., below the PTCDA molecules. This conjecture is supported by work function data<sup>23</sup> and finally proven by NIXSW measurements of the vertical position of K atoms with respect to Ag Bragg planes.<sup>23</sup>

We first discuss the work function data. Before annealing the K/PTCDA/Ag(110) interface, potassium is already in a partially ionic state, because the binding energy of the K  $2p_{3/2}$  core level, 294 eV, is close to the one of  $\text{K}^+$  (294.5 eV).<sup>32</sup> At this stage, potassium is distributed in a disordered way above or within the molecular layer. This is confirmed by the significant increase of the secondary electron intensity in UPS<sup>23,33</sup> after potassium deposition and by the lack of potassium-associated long-range order in LEED images. The positive charge of potassium and its negative image charge in the metal generate a contribution to the surface dipole that is responsible for a work function decrease of approximately 0.9 eV. Upon annealing of K/PTCDA/Ag(110), the long-range ordered stripe phase forms [Fig. 2(d)], in which, judging from the decreased intensity of secondary electrons, K atoms are now better ordered (see STM data discussed below). At the same time, the work function increases again by approximately 0.3 eV, suggesting that potassium moves towards the metal, thereby increasing the

total surface dipole again.<sup>34</sup> This rearrangement is also implied by a 0.3 eV decrease of the K  $2p_{3/2}$  binding energy, indicating an improved screening of the core hole by the metal. In fact, NIXSW experiments, in which we find a vertical position of K atoms coinciding with the Bragg planes, prove that in the stripe phase K atoms are at the same vertical positions of the Ag atoms [Fig. 1(c)].<sup>23</sup>

Knowing that potassium is located in the Ag surface, we search for it in STM by applying special imaging conditions. Namely, we image the stripe phase with a bias voltage that probes a K resonance known from inverse photoemission spectroscopy of K/Ag(110).<sup>35</sup> The corresponding STM image in Fig. 2(e) shows a periodic array of bright lobes within and across the up and down terraces. We attribute these features, which are absent for PTCDA/Ag(110), to the K atoms lying beneath the PTCDA molecules in the topmost Ag layer. Interestingly, STM shows that K atoms are located near the O atoms of PTCDA. This finding is confirmed by O 1s and C 1s core level spectra.<sup>23</sup> In going from the K-free PTCDA/Ag(110) brick-wall phase [Fig. 2(b)] to the stripe phase, the binding energies of O 1s and C 1s core levels shift by +0.6 eV ( $O_{\text{carb}}$ ), +0.8 eV ( $O_{\text{anhyd}}$ ), and +0.4 eV ( $C_{\text{peryl}}$ ); this can be explained by the presence of positively charged potassium in the vicinity of the PTCDA molecules (see below).

Concluding so far, the unambiguous evidence that potassium is both in the silver surface plane and located close to the oxygens of PTCDA confirms the feasibility of selectively separating O atoms of PTCDA from silver by inserting K atoms into the Ag(110) surface. Therefore, our goal to manipulate the oxygen bonding channel is indeed achieved [for this reason we refer to the stripe phase as PTCDA/K:Ag(110) from now on; a structure model is shown in Fig. 3], and we investigate now the effect of this local modification on the overall bonding of PTCDA to Ag(110), and in particular on the perylene core.

The molecular geometry in the PTCDA/K:Ag(110) system is shown in Fig. 1(c). Carboxylic and anhydride oxygens

TABLE I. Adsorption heights in Å with respect to the unrelaxed uppermost Ag layer as determined by NIXSW (Refs. 22 and 23). The numbers for PTCDA/Ag(110) differ slightly from those given in Ref. 12, although within the quoted experimental errors, because a different fitting program (TORRICELLI) was used.<sup>22,30</sup>

	PTCDA/Ag(110)	PTCDA/K:Ag(110)
$C_{\text{peryl}}$	$2.59 \pm 0.01$	$2.64 \pm 0.03$
$C_{\text{func}}$	$2.45 \pm 0.11$	$2.73 \pm 0.06$
$O_{\text{carb}}$	$2.32 \pm 0.05$	$2.63 \pm 0.10$
$O_{\text{anhyd}}$	$2.41 \pm 0.06$	$2.76 \pm 0.11$

together with the functional carbons lift by approximately 0.30 Å as compared to PTCDA/Ag(110). This indicates a dramatic change of the oxygen-metal interaction. The K- $O_{\text{anhyd}}$  distance of approximately 2.80 Å (see Table I and Fig. 3) is consistent with calculations for K-PTCDA crystals, which reveal a K<sup>+</sup> ion coordinated by four carboxylic oxygens with K-O distances ranging from 2.55 to 3.00 Å.<sup>31</sup> We note that typical K-O bonding distances amount to 2.51 Å<sup>36</sup> in the KO<sub>2</sub> molecule and to 2.71 Å<sup>36,37</sup> or 2.92 Å<sup>37</sup> in the KO<sub>2</sub> crystal.

In contrast to the behavior of the O atoms, the perylene core changes its adsorption height by only 0.05 Å [Fig. 1(c)]. The direction of this change is consistent with the bonding model of Ref. 12 described above: Because the oxygen atoms move to a position higher than the perylene core, the perylene core can no longer be pulled by the functional groups into the repulsive interaction with the silver surface, and hence it must relax upwards, too, which indeed it does. However, its upward relaxation is much smaller than the shift of the oxygens. This is a direct indication for the existence of an attractive interaction between the perylene core and the silver substrate ( $C_{\text{peryl}}$ -Ag bonding channel). Therefore, for the PTCDA/K:Ag(110) system the existence of two bonding channels<sup>12</sup> is proven by the present NIXSW results.

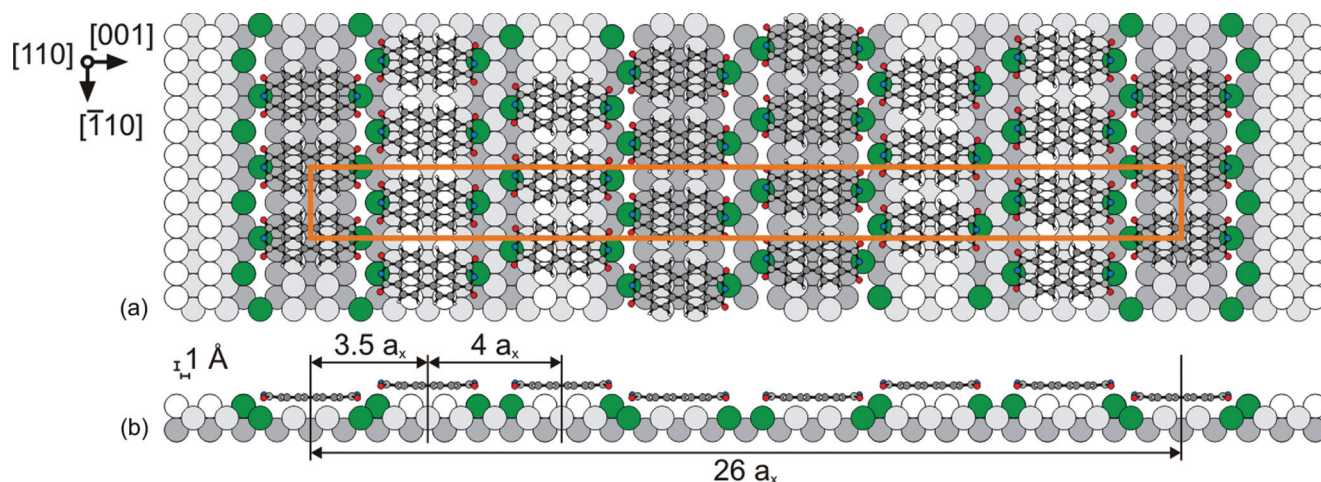


FIG. 3. (Color) Top (a) and side (b) view of the structure model of the PTCDA/K:Ag(110) stripe phase based on STM and SPA-LEED data ( $a_x = 4.09$  Å). The unit cell ( $3 \ 0 \ | \ 0 \ 26$ ) is marked in orange. SPA-LEED, STM, and angle-resolved UPS data indicate a small tilt ( $2^\circ - 7^\circ$ ) of the molecules away from the [001] direction. Positions of K atoms (green) along  $[\bar{1}10]$  and of PTCDA molecules relative to the substrate along  $[\bar{1}10]$  are not known, but XPS data suggest the largest influence of K atoms on  $O_{\text{anhyd}}$ . Hence, molecules have been placed such that  $O_{\text{anhyd}}$  are on top of K.

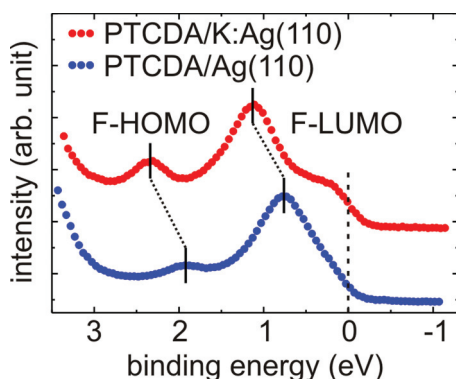


FIG. 4. (Color) UPS data of PTCDA/Ag(110) and PTCDA/K:Ag(110) integrated over the polar angle interval  $[1^\circ, 60^\circ]$  with the azimuthal angle fixed along the  $[\bar{1}10]$  direction of the substrate (Ref. 23).

The question now arises as to whether the existence of the  $C_{\text{peryl}}\text{-Ag}$  bonding channel can be transferred to the bonding of PTCDA on the *pure* Ag(110) surface. We know from our structural investigations (see above) that the geometric structure below the perylene core is *not* affected by potassium. By comparing the electronic structures of the PTCDA/K:Ag(110) and PTCDA/Ag(110) interfaces we now show that the bonding situation of the perylene core is comparable for the two interfaces.

Figure 4 shows UPS data for the two interfaces.<sup>23</sup> On incorporation of potassium, both the former highest occupied molecular orbital (F-HOMO) and the F-LUMO shift to larger binding energies (F-LUMO: 0.78 eV  $\rightarrow$  1.14 eV; F-HOMO: 1.91 eV  $\rightarrow$  2.38 eV). We note that this shift is nearly rigid (to within 0.11 eV). We can explain all observed binding energy shifts, including those of core levels which were mentioned earlier, by the electrostatic field which is produced by the positively charged potassium and which acts on the photoelectrons from PTCDA, either by an initial or a final state effect or a combination thereof. The initial state effect is connected to the potassium-induced electric potential at the positions of the PTCDA molecules, which increases the energy required to remove an electron to infinity, while the final state effect arises because the positive charge of the potassium freezes the surrounding electronic charge density which therefore becomes less effective in screening the photohole left behind the emitted photoelectron, leading to an increased binding energy. We note that the shift of the C  $1s_{\text{peryl}}$  core level (0.4 eV) is approximately equal to the ones of F-LUMO (0.36 eV)

and F-HOMO (0.47 eV), which follows naturally, because the photohole of both frontier orbitals is localized mainly on the perylene core of the molecule. Moreover, on the basis of our structural model in Fig. 3 we expect that the XPS binding energy shifts are larger for  $O_{\text{carb}}$  atoms than for C atoms, and yet larger for  $O_{\text{anhyd}}$ , in agreement with our experimental results.<sup>23</sup> The fact that the binding energy shift of the F-LUMO is slightly smaller than that of the F-HOMO can be explained by the 0.05 Å upward relaxation of the perylene core, which is coupled to a decreasing F-LUMO binding energy.<sup>12</sup> The analysis of the electronic structure hence suggests that the existence of the  $C_{\text{peryl}}\text{-Ag}$  channel can be transferred from PTCDA/K:Ag(110), where we have observed it directly, to PTCDA/Ag(110), although details may be different due to the electronic synergism between the two channels.<sup>12</sup> The existence of the  $C_{\text{peryl}}\text{-Ag}$  channel for PTCDA/Ag(110) is also confirmed by a density functional theory calculation including a semiempirical van der Waals correction which reveals an enhanced charge density between the perylene core and the Ag(110) surface.<sup>12</sup>

In conclusion, we have successfully achieved the selective local modification of *one* bonding channel of a functionalized organic molecule, by local substitution of potassium into the metal surface. We have proven that on Ag(110) both bonding channels of PTCDA that are discussed in Ref. 12 indeed exist. Moreover, we have observed a moderate coupling between the bonding heights of the functional groups and the perylene core, showing that both channels influence each other. We anticipate that the approach taken here to analyzing the surface bonding of multifunctional adsorbates is of general validity. Because of the distinct affinities of the two bonding channels towards chemically different regions of the reconstructed Ag(110) surface, the periodicity of the missing row reconstruction in the PTCDA/K:Ag(110) system is defined by the geometry of PTCDA. By tuning the length of the carbon backbone of the molecule, the period of reconstruction can hence be controlled effectively.

We thank J. Zegenhagen, B. Detlefs, and Y. Mi (ESRF), M. Ostler and T. Seyller (Universität Erlangen-Nürnberg), M. Buchholz (Universität Bonn), E. M. Reinisch, T. Ules, G. Koller, and M. G. Ramsey (Universität Graz) for helpful discussions and experimental support at the ESRF and BESSY II. Financial support by the ESRF and the DFG under Projects No. SFB 624, No. SFB 813, No. SO 407/6-1, and No. TA 244/3-2 is acknowledged. T.S. acknowledges the Alexander von Humboldt foundation for financial support.

\*g.mercurio@fz-juelich.de

<sup>1</sup>J. V. Barth, *Annu. Rev. Phys. Chem.* **58**, 375 (2007).

<sup>2</sup>H.-J. Gao and L. Gao, *Prog. Surf. Sci.* **85**, 28 (2010).

<sup>3</sup>J. Hwang, A. Wan, and A. Kahn, *Mater. Sci. Eng., R* **64**, 1 (2009).

<sup>4</sup>N. Koch, *J. Phys.: Condens. Matter* **20**, 184008 (2008).

<sup>5</sup>F. S. Tautz, *Prog. Surf. Sci.* **82**, 479 (2007).

<sup>6</sup>A. Gerlach, S. Sellner, F. Schreiber, N. Koch, and J. Zegenhagen, *Phys. Rev. B* **75**, 045401 (2007).

<sup>7</sup>S. Duhm, A. Gerlach, I. Salzmann, B. Broeker, R. Johnson, F. Schreiber, and N. Koch, *Org. Electron.* **9**, 111 (2008).

<sup>8</sup>L. Romaner, D. Nabok, P. Puschnig, E. Zojer, and C. Ambrosch-Draxl, *New J. Phys.* **11**, 053010 (2009).

<sup>9</sup>A. Abbasi and R. Scholz, *J. Phys. Chem. C* **113**, 19897 (2009).

<sup>10</sup>M. Marks, N. L. Zaitsev, B. Schmidt, C. H. Schwalb, A. Schöll, I. A. Nechaev, P. M. Echenique, E. V. Chulkov, and U. Höfer, *Phys. Rev. B* **84**, 081301 (2011).

- <sup>11</sup>V. G. Ruiz, W. Liu, E. Zojer, M. Scheffler, and A. Tkatchenko, *Phys. Rev. Lett.* **108**, 146103 (2012).
- <sup>12</sup>O. Bauer, G. Mercurio, M. Willenbockel, W. Reckien, C. H. Schmitz, B. Fiedler, S. Soubatch, T. Bredow, F. S. Tautz, and M. Sokolowski, *Phys. Rev. B* **86**, 235431 (2012).
- <sup>13</sup>Y. Zou, L. Kilian, A. Schöll, T. Schmidt, R. Fink, and E. Umbach, *Surf. Sci.* **600**, 1240 (2006).
- <sup>14</sup>M. Wießner, D. Hauschild, A. Schöll, F. Reinert, V. Feyer, K. Winkler, and B. Krömker, *Phys. Rev. B* **86**, 045417 (2012).
- <sup>15</sup>J. Zirossoff, F. Forster, A. Schöll, P. Puschnig, and F. Reinert, *Phys. Rev. Lett.* **104**, 233004 (2010).
- <sup>16</sup>P. Puschnig, E.-M. Reinisch, T. Ules, G. Koller, S. Soubatch, M. Ostler, L. Romaner, F. S. Tautz, C. Ambrosch-Draxl, and M. G. Ramsey, *Phys. Rev. B* **84**, 235427 (2011).
- <sup>17</sup>M. Eremtchenko, J. A. Schaefer, and F. S. Tautz, *Nature (London)* **425**, 602 (2003).
- <sup>18</sup>M. Rohlfiger, R. Temirov, and F. S. Tautz, *Phys. Rev. B* **76**, 115421 (2007).
- <sup>19</sup>A. Hauschild, K. Karki, B. C. C. Cowie, M. Rohlfiger, F. S. Tautz, and M. Sokolowski, *Phys. Rev. Lett.* **94**, 036106 (2005).
- <sup>20</sup>A. Hauschild, R. Temirov, S. Soubatch, O. Bauer, A. Schöll, B. C. C. Cowie, T.-L. Lee, F. S. Tautz, and M. Sokolowski, *Phys. Rev. B* **81**, 125432 (2010).
- <sup>21</sup>L. Kilian, A. Hauschild, R. Temirov, S. Soubatch, A. Schöll, A. Bendounan, F. Reinert, T.-L. Lee, F. S. Tautz, M. Sokolowski, and E. Umbach, *Phys. Rev. Lett.* **100**, 136103 (2008).
- <sup>22</sup>G. Mercurio, O. Bauer, M. Willenbockel, N. Fairley, W. Reckien, C. H. Schmitz, B. Fiedler, S. Soubatch, T. Bredow, M. Sokolowski, and F. S. Tautz, *Phys. Rev. B* **87**, 045421 (2013).
- <sup>23</sup>See Supplemental Material at <http://link.aps.org/supplemental/10.1103/PhysRevB.87.121409> for more details.
- <sup>24</sup>V. Shklover, S. Schmitt, E. Umbach, F. S. Tautz, M. Eremtchenko, Y. Shostak, J. Schaefer, and M. Sokolowski, *Surf. Sci.* **482–485**, 1241 (2001).
- <sup>25</sup>S. Schmidt, diploma thesis, Julius-Maximilians-Universität Würzburg, 1998.
- <sup>26</sup>*Physics and Chemistry of Alkali Metal Adsorption, Materials Science Monographs*, edited by H. P. Bonzel, A. M. Bradshaw, and G. Ertl, Vol. 57 (Elsevier Science, Amsterdam, 1989).
- <sup>27</sup>H. Tochihara and S. Mizuno, *Prog. Surf. Sci.* **58**, 1 (1998).
- <sup>28</sup>B. E. Hayden, K. C. Prince, P. J. Davie, G. Paolucci, and A. M. Bradshaw, *Solid State Commun.* **48**, 325 (1983).
- <sup>29</sup>F. Moresco, M. Rocca, T. Hildebrandt, V. Zielasek, and M. Henzler, *Surf. Sci.* **424**, 62 (1999).
- <sup>30</sup>TORRICELLI is an XSW data analysis and simulation program written by G. Mercurio, copies can be obtained from [s.tautz@fz-juelich.de](mailto:s.tautz@fz-juelich.de).
- <sup>31</sup>C. Zazza, S. Meloni, A. Palma, M. Knupfer, G. G. Fuentes, and R. Car, *Phys. Rev. Lett.* **98**, 046401 (2007).
- <sup>32</sup>M. De Seta and F. Evangelisti, *Phys. Rev. B* **51**, 1096 (1995).
- <sup>33</sup>T. Sueyoshi, H. Kakuta, M. Ono, K. Sakamoto, S. Kera, and N. Ueno, *Appl. Phys. Lett.* **96**, 093303 (2010).
- <sup>34</sup>U. Martinez, L. Giordano, and G. Pacchioni, *J. Chem. Phys.* **128**, 164707 (2008).
- <sup>35</sup>W. Jacob, E. Bertel, and V. Dose, *Phys. Rev. B* **35**, 5910 (1987).
- <sup>36</sup>Y. N. Zhuravlev, N. G. Kravchenko, and O. S. Obolonskaya, *Russ. J. Phys. Chem. B* **4**, 20 (2010).
- <sup>37</sup>S. C. Abrahams and J. Kalnajs, *Acta Crystallogr.* **8**, 503 (1955).